doi:10.1038/nature08964

LETTERS

Native $GABA_B$ receptors are heteromultimers with a family of auxiliary subunits

Jochen Schwenk[1]*, Michaela Metz[2]*, Gerd Zolles[1]*, Rostislav Turecek[2,6]*, Thorsten Fritzius[2], Wolfgang Bildl[1], Etsuko Tarusawa[4], Akos Kulik[4], Andreas Unger[4], Klara Ivankova[2], Riad Seddik[2], Jim Y. Tiao[2], Mathieu Rajalu[2], Johana Trojanova[6], Volker Rohde[3], Martin Gassmann[2], Uwe Schulte[1,3], Bernd Fakler[1,5] & Bernhard Bettler[2]

$GABA_B$ receptors are the G-protein-coupled receptors for γ-aminobutyric acid (GABA), the main inhibitory neurotransmitter in the brain. They are expressed in almost all neurons of the brain, where they regulate synaptic transmission and signal propagation by controlling the activity of voltage-gated calcium (Ca_v) and inward-rectifier potassium (K_{ir}) channels[1]. Molecular cloning revealed that functional $GABA_B$ receptors are formed by the heteromeric assembly of $GABA_{B1}$ with $GABA_{B2}$ subunits[2–5]. However, cloned $GABA_{B(1,2)}$ receptors failed to reproduce the functional diversity observed with native $GABA_B$ receptors[6–8]. Here we show by functional proteomics that $GABA_B$ receptors in the brain are high-molecular-mass complexes of $GABA_{B1}$, $GABA_{B2}$ and members of a subfamily of the KCTD (potassium channel tetramerization domain-containing) proteins. KCTD proteins 8, 12, 12b and 16 show distinct expression profiles in the brain and associate tightly with the carboxy terminus of $GABA_{B2}$ as tetramers. This co-assembly changes the properties of the $GABA_{B(1,2)}$ core receptor: the KCTD proteins increase agonist potency and markedly alter the G-protein signalling of the receptors by accelerating onset and promoting desensitization in a KCTD-subtype-specific manner. Taken together, our results establish the KCTD proteins as auxiliary subunits of $GABA_B$ receptors that determine the pharmacology and kinetics of the receptor response.

To test the hypothesis that functional diversity of native $GABA_B$ receptors results from additional as yet unknown subunits, a proteomic analysis was performed with a recently developed approach combining affinity purification of protein complexes and quantitative mass spectrometry[9–11]. For affinity purifications, antibodies specific for $GABA_{B1}$ (anti-$GABA_{B1}$ targeting $GABA_{B1a}$ and $GABA_{B1b}$) or $GABA_{B2}$ (anti-$GABA_{B2}$) were used on appropriately solubilized membrane fractions from total rat and mouse brains; $GABA_B$ receptors in these protein preparations showed high molecular masses of more than about 0.7 MDa (Fig. 1a, c). Total eluates of anti-$GABA_B$ affinity purifications from brain membranes of rats and wild-type mice as well as of mice with genetic deletions of $GABA_{B1}$ and $GABA_{B2}$ subunits[12–14] were analysed by high-resolution nanoflow liquid chromatography tandem mass spectrometry (Supplementary Figs 1–3) that provided both the identity and amount of proteins[10,15]. As shown in Fig. 1b, both $GABA_{B1}$ and $GABA_{B2}$ were purified by either anti-$GABA_B$ antibody at high yield; the large numbers of peptides retrieved by mass spectrometry covered 69% and 61%, respectively, of the accessible primary sequences (Supplementary Fig. 4 and Supplementary Tables 1 and 2). Normalization of the peak volumes to the number of mass-spectrometry-accessible amino acids (normalized abundance) showed that $GABA_{B1}$ and $GABA_{B2}$ were present in both anti-$GABA_B$ affinity purifications at comparable molar ratios (Fig. 1b). In addition to $GABA_{B1}$ and $GABA_{B2}$, our mass spectrometry analyses identified the KCTD proteins 8, 12, 12b and 16, four closely related members of a large family of soluble proteins (21 and 22 different genes in the human and mouse genomes, respectively) that share conserved domains in their amino termini (T1 domain, homology to K_v-type K^+ channels) and carboxy termini (C-terminal domain; Fig. 1b and Supplementary Fig. 5). KCTD proteins 8, 12 and 16 were co-purified with both anti-$GABA_B$ antibodies at similarly high yields to those of $GABA_{B1}$ and $GABA_{B2}$ (Fig. 1b and Supplementary Fig. 3; sequence coverages of 79%, 97% and 80%, respectively; details in Supplementary Fig. 4 and Supplementary Tables 1 and 2), whereas KCTD12b was retrieved in markedly smaller amounts. No KCTD-specific peptides were detected in affinity purifications with anti-$GABA_{B1}$ and anti-$GABA_{B2}$ from brains of $GABA_{B1}^{-/-}$ and $GABA_{B2}^{-/-}$ knockout mice, respectively. In addition, KCTD proteins were not retrieved in anti-$GABA_{B1}$ affinity purifications from $GABA_{B2}^{-/-}$ brains, in which mass spectrometry analyses detected considerable amounts of $GABA_{B1}$ protein (Supplementary Fig. 3). These results strongly suggested that the KCTD proteins 8, 12, 12b and 16 are integral constituents of native $GABA_B$ receptors through interaction with the $GABA_{B2}$ subunit.

Co-assembly of the identified KCTD proteins with native $GABA_B$ receptors was corroborated by reverse affinity purifications with antibodies specific for either KCTD12 or KCTD16 (anti-KCTD12, anti-KCTD16; Supplementary Fig. 6). Both anti-KCTD antibodies effectively co-purified $GABA_{B1}$ and $GABA_{B2}$ as well as the other KCTD proteins (Supplementary Fig. 3b); the two $GABA_B$ receptor core subunits were the most abundantly co-purified proteins and the only G-protein-coupled receptor subunits detected by mass spectrometry. The KCTD–$GABA_B$ co-assembly was further confirmed by western blot analysis of native gel separations of brain membrane fractions (Fig. 1c). Both KCTD12 and KCTD16 co-migrated strictly with the $GABA_{B1}$ and $GABA_{B2}$ core subunits, although their signals showed only partial overlap with each other. This suggests that a portion of both KCTDs may be integrated into the same $GABA_B$ complexes, and the remaining KCTD proteins participate in distinct $GABA_B$ receptors of either higher (KCTD16) or lower (KCTD12) molecular size (Fig. 1c). All $GABA_B$ receptors resolved on native gels seemed to be associated with the KCTD proteins and markedly exceeded the molecular mass predicted for $GABA_{B(1,2)}$ heterodimers (about 240 kDa).

Direct co-assembly of KCTD proteins with the $GABA_{B2}$ subunit was finally demonstrated in affinity purifications from membrane

[1]Institute of Physiology II, University of Freiburg, Engesserstrasse 4, 79108 Freiburg, Germany. [2]Department of Biomedicine, Institute of Physiology, Pharmazentrum, University of Basel, Klingelbergstrasse 50/70, CH-4056 Basel, Switzerland. [3]Logopharm GmbH, Engesserstrasse 4, 79108 Freiburg, Germany. [4]Institute of Anatomy and Cell Biology, University of Freiburg, Albertstrasse 23, 79104 Freiburg, Germany. [5]Center for Biological Signaling Studies (bioss), Albertstrasse 10, 79104 Freiburg, Germany. [6]Institute of Experimental Medicine, Academy of Sciences of the Czech Republic, Videnska 1083, 14220-Prague 4, Czech Republic.
*These authors contributed equally to this work.

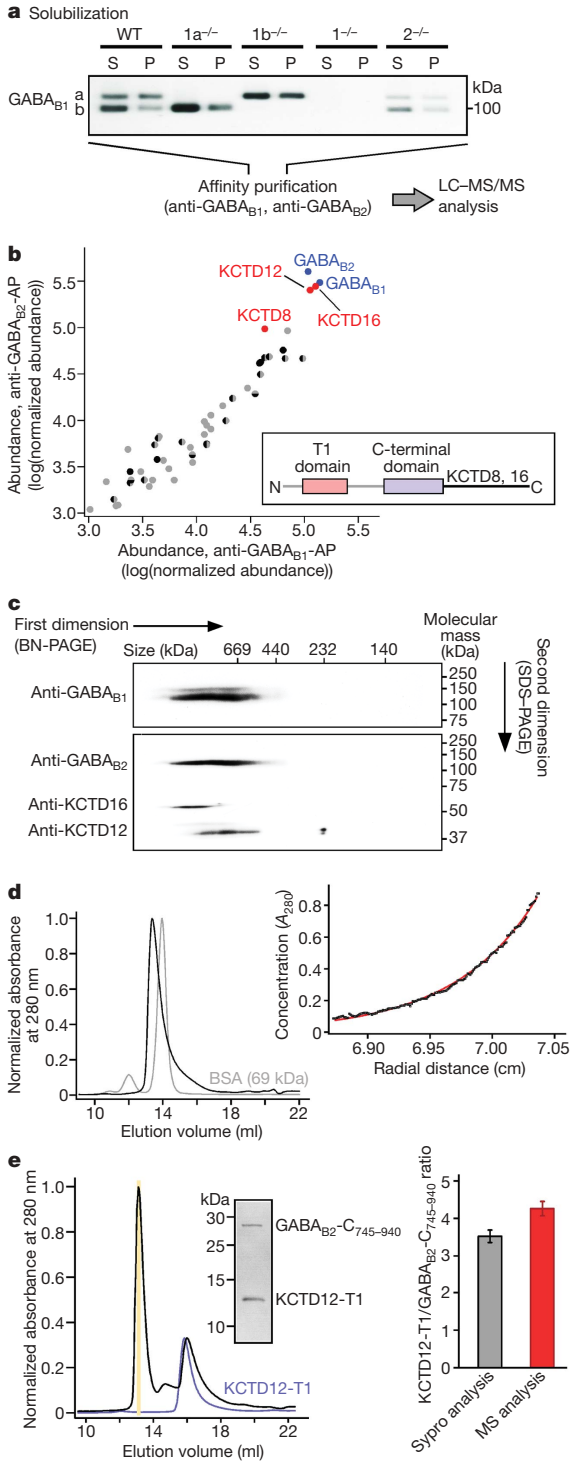

Figure 1 | Identification of four KCTD proteins as subunits of native GABA$_B$ receptors. a, Input and scheme of the proteomic approach used. SDS–PAGE separation of solubilized (S) and insoluble (P) protein fractions obtained with the CL-91 buffer from brain membranes of wild-type (WT) and the indicated knockout mice western blotted with anti-GABA$_{B1}$. **b**, Normalized abundance values of proteins in affinity purifications (AP) with anti-GABA$_{B1}$ and anti-GABA$_{B2}$. Grey circles denote background proteins, filled circles indicate proteins specifically co-purified with both antibodies, half-filled symbols represent proteins specifically co-purified with one antibody (left side filled with anti-GABA$_{B2}$, lower half filled with anti-GABA$_{B1}$). Inset: conserved domains of KCTD proteins. **c**, Two-dimensional gel separation of solubilized GABA$_B$ receptors from rat brain western blotted with the indicated antibodies. Size (blue native (BN)–PAGE) and molecular mass (SDS–PAGE) as indicated. **d**, SEC of the GB1-tagged KCTD12-T1; BSA added for reference. Inset: sedimentation equilibrium analysis of the monodisperse SEC fraction of GB1-tagged KCTD12-T1 (molecular mass 20.4 kDa); data were obtained with a protein concentration of 0.5 mg ml^{-1} at 12,000 r.p.m. The continuous line is a fit of the data yielding a molecular mass of 81.2 kDa. **e**, Left: SEC analysis of the KCTD12-T1 + GABA$_{B2}$-C$_{745–940}$ complex; purified KCTD12-T1 added for comparison. Inset: SDS–PAGE of the indicated SEC fraction (yellow bar) stained with Sypro Orange. Right: stoichiometry of the complex constituents obtained from fluorescence intensity measurements (Sypro analysis) or from quantitative mass spectrometry analyses of gel separations as in the inset; data are means and s.d. for three experiments.

fractions of HEK293 cells expressing various combinations of differentially tagged GABA$_{B1}$, GABA$_{B2}$ and KCTD12 proteins (Supplementary Fig. 7a). Subsequent analysis showed that GABA$_{B2}$ and KCTD proteins interact through the T1 domain and the C terminus of GABA$_{B2}$, in which a six-residue stretch (901–906) with an aromatic residue at position 902 was found to be of particular importance (Supplementary Fig. 7b, c). To determine the stoichiometry of this assembly, the T1 domain of KCTD12 (KCTD12-T1) as well as complexes of KCTD12-T1 and the full-length C terminus of GABA$_{B2}$ (KCTD12-T1 + GABA$_{B2}$-C$_{745–940}$) were analysed by size-exclusion chromatography (SEC), analytical ultracentrifugation and quantitative mass spectrometry. As shown in Fig. 1d, the tagged KCTD12-T1 eluted as a monodisperse protein fraction in SEC, and in subsequent sedimentation equilibrium analyses it showed a molecular mass of 82.9 ± 4.3 kDa (mean ± s.d. for four runs), a value very close to that calculated for a tetramer of tagged KCTD12-T1 proteins. Similarly, analysis of the subunit stoichiometry of the KCTD12-T1–GABA$_{B2}$-C$_{745–940}$ complex by mass spectrometry-based or fluorescence-based quantification revealed a KCTD12-T1:GABA$_{B2}$-C$_{745–940}$ ratio of about 4:1 (Fig. 1e). This result confirmed the tetrameric assembly of KCTD12-T1 and suggested that each KCTD-T1 tetramer offers one binding site for the C terminus of GABA$_{B2}$. When related to the size on native gels (Fig. 1c), this arrangement suggests that native GABA$_B$ receptors are most probably dimeric assemblies[16] of units composed of GABA$_{B1}$, GABA$_{B2}$ and a KCTD tetramer (estimated unit molecular mass of about 350–400 kDa).

Next, the expression profiles of the identified KCTD proteins in the brain were investigated by *in situ* hybridization. As illustrated in Fig. 2a, the four KCTDs showed distinct but partly overlapping expression patterns. The subcellular distribution of KCTD proteins 12 and 16 was assessed in pre-embedding immunoelectron microscopy and in immunolabelling of freeze–fracture replicas of the hippocampal CA1 region. Both techniques localized the anti-KCTD12 and anti-KCTD16 immunoreactivity to the plasma membrane of presynaptic and postsynaptic compartments of principal cells that were also stained by anti-GABA$_{B1}$ (Fig. 2b, c). In all locations, immunoparticles showed a similarly clustered organization for GABA$_{B1}$, KCTD12 and KCTD16 (Fig. 2b, c and Supplementary Fig. 8), which is consistent with the known clustering of native GABA$_B$ receptors[17] and their heteromultimeric assembly from these subunits reported here.

To test whether co-assembled KCTD proteins alter the functional properties of GABA$_B$ receptors, GABA$_{B(1,2)}$ or GABA$_{B(1,2)}$-KCTD heteromultimers were co-expressed in *Xenopus* oocytes or Chinese hamster ovary (CHO) cells together with the Gβγ-regulated effector ion channels K$_{ir}$3 or Ca$_v$2.1/Ca$_v$2.2 (corresponding to P/Q-type and N-type channels). Figure 3a shows typical current traces recorded in whole oocytes from heteromeric K$_{ir}$3.1/3.2 channels in response to 60-s applications of GABA to GABA$_B$ receptors assembled from GABA$_{B1}$ and GABA$_{B2}$ (GABA$_B$) either alone or in combination with KCTD proteins (GABA$_B$ + KCTDx). Although all receptor types effectively activated K$_{ir}$3 channels, the respective K^+ currents markedly differed in their time courses: currents activated by GABA$_B$ + KCTD16 and GABA$_B$ + KCTD8 decreased only slightly over the application period, very similarly to those elicited by GABA$_B$ alone, whereas the responses of both GABA$_B$ + KCTD12 and GABA$_B$ + KCTD12b receptors showed pronounced desensitization (more than 70% of maximum; $P < 0.001$,

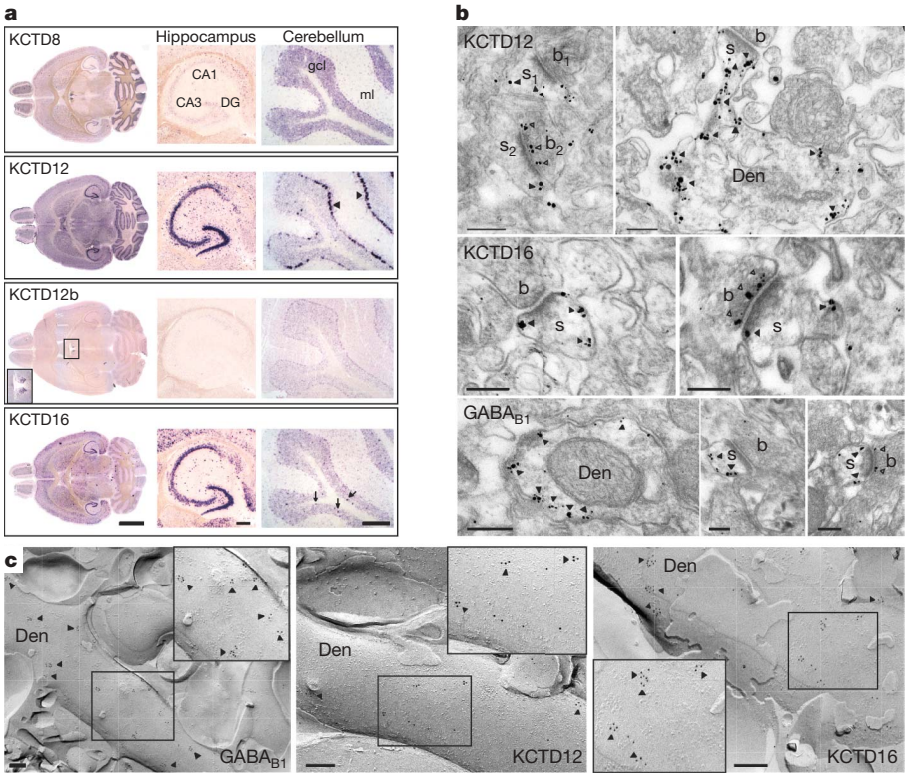

Figure 2 | Expression profile and subcellular localization of KCTD proteins in the brain. **a**, *In situ* hybridizations with digoxigenin-labelled antisense probes on horizontal sections of the medial tier (overview (left), hippocampal formation (middle) and cerebellum (right)) of adult mouse brains. DG, dentate gyrus; gcl, granule cell layer; ml, molecular cell layer; arrows and arrowheads denote cerebellar Golgi/Purkinje cells. KCTD12b transcripts are restricted to the medial habenula (rectangular frame, enlarged in inset). Scale bars, 200 μm (overviews) and 40 μm (hippocampus and cerebellum). **b**, Immunoreactivities for the indicated KCTDs and $GABA_{B1}$ in the stratum radiatum of the hippocampal CA1 region detected by pre-embedding immunogold electron microscopy. Immunogold particles were most abundant at the extrasynaptic plasma membrane (filled arrowheads) of dendritic spines (s, s_1, s_2) and dendritic shafts (Den) of pyramidal cells, but also found at the presynaptic membranes (open arrowheads) of boutons (b, b_1, b_2) of putative excitatory cells. **c**, Clusters of $GABA_{B1}$ and KCTD proteins (arrowheads) over the surface of dendrites (Den) of CA1 pyramidal cells assessed by SDS-digested freeze–fracture replica immunolabelling. Insets are enlargements of the indicated frames. Scale bars, 0.2 μm (**b**, **c**).

Dunnett's multiple comparison test; Fig. 3a, c and Supplementary Fig. 9). The extent of the KCTD12-induced desensitization was essentially independent of the agonist concentration in the range 10 μM to 1 mM and required two exponential functions for adequate description (Fig. 3c). The results on KCTD subtype-specific properties of $GABA_B$-receptor signalling were closely reproduced when the $K_{ir}3$ channels were replaced by $Ca_v2.1$ or $Ca_v2.2$ channels as effector systems. Thus, whereas activation of $GABA_B$, $GABA_B$ + KCTD16 or $GABA_B$ + KCTD8 led to stable inhibition of the Ca_v channels over the application period, activated $GABA_B$ + KCTD12 or $GABA_B$ + KCTD12b receptors decreased the Ca_v channel activity only transiently, reflecting the pronounced receptor desensitization (Fig. 3b, c). The KCTD12-induced desensitization was specific for $GABA_B$ receptors and was not observed when $GABA_{B2}$(Y902A), a mutant precluding KCTD binding, was co-assembled into the receptor complexes (Supplementary Fig. 10).

Another set of experiments used CHO cells because they permit faster solution exchange (time constant of about 12 ms), lack endogenous expression of KCTD proteins and offer a different cellular background for G-protein signalling. $GABA_B$-activated $K_{ir}3$ currents elicited by 25-s applications of baclofen closely recapitulated the pronounced differences in kinetics and extent of desensitization seen with the four KCTD proteins in oocytes (Fig. 4a). In particular, approximation of the KCTD12-induced desensitization by exponential functions required two components with time constants of 1.5 ± 0.4 s (mean ± s.d., $n = 10$; relative contribution of 0.42 ± 0.14) and 8.9 ± 2.1 s (relative contribution of 0.58 ± 0.14). Moreover, the rapid solution exchange resolving the onset and activation phases of the receptor responses indicated that all four KCTD proteins markedly accelerated the $GABA_B$ response, although to different extents. The values determined for the 20–80% rise time of the $K_{ir}3$ currents revealed that KCTD8 speeded the activation about threefold, whereas KCTD12 accelerated it almost tenfold ($P < 0.001$, Dunnett's multiple comparison test; Fig. 4b). In addition to their impact on the kinetics, KCTDs 12 and 16 significantly influenced the agonist concentration dependence of the $GABA_B$ responses as determined by apparent dose–response relationships with baclofen. Thus, KCTD12 and KCTD16 shifted the respective concentrations giving half-maximal response (half-maximum effective concentration (EC_{50}) values; fitted to the mean currents) towards lower concentrations by factors of about 7 and 3, respectively (Fig. 4c).

Finally, the KCTD effects were examined in cultured hippocampal neurons, which show robust $K_{ir}3$-mediated $GABA_B$ responses[18] and express KCTD proteins 8, 12 and 16 (Supplementary Fig. 11). Accordingly, K^+ currents elicited by rapid baclofen application (time constant of about 22 ms) showed values for the 20–80% rise time of 0.36 ± 0.11 s ($n = 26$) and a steady-state desensitization of 34 ± 9% ($n = 38$; Fig. 4d). On transfection with the four KCTD proteins, a significant increase in steady-state desensitization was obtained with KCTDs 12 and 12b only ($P < 0.001$, Dunnett's multiple comparison test; Fig. 4d). Moreover, KCTDs 12 and 12b also induced a significant decrease in the 20–80% rise time (0.16 ± 0.05 s ($n = 11$) and 0.21 ± 0.05 s ($n = 7$); Fig. 4d). These effects of KCTD proteins on $GABA_B$ receptors in hippocampal neurons were corroborated by a dominant-negative transgenic approach and short hairpin RNA (shRNA)-mediated knockdown of KCTD protein. Thus, both expression of a mutant $GABA_{B2}$ lacking the KCTD-binding site in $GABA_{B2}^{-/-}$ neurons and knockdown of KCTD12 in wild-type neurons led to a significant decrease in desensitization and a slowed onset of the

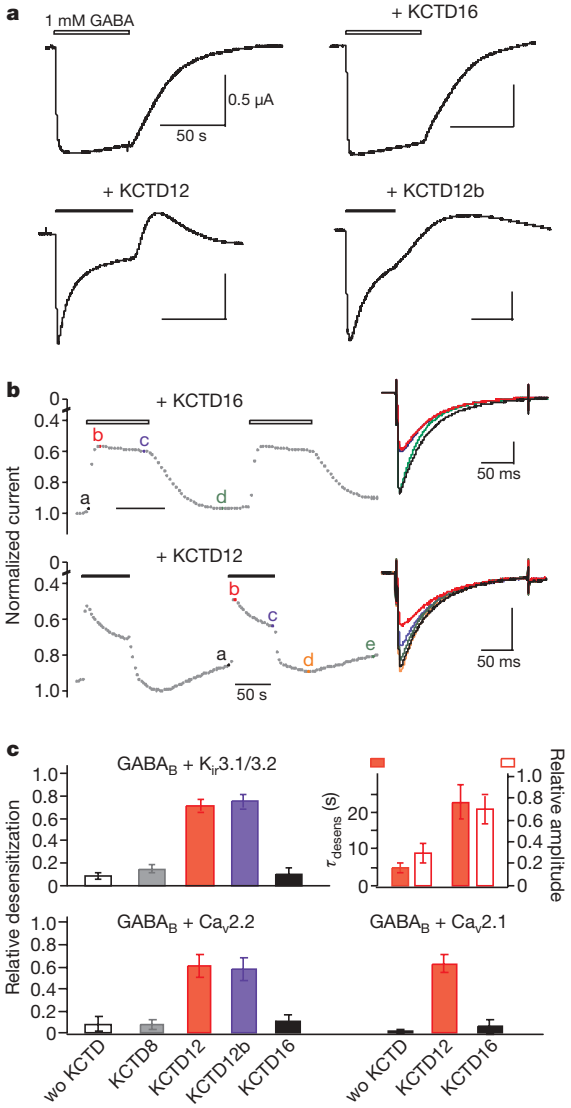

Figure 3 | G-protein signalling of GABA$_B$ receptors is determined by KCTD proteins. **a**, K^+ currents recorded at −50 mV in response to GABA applications (1 mM) from whole *Xenopus* oocytes co-expressing GABA$_B$, K$_{ir}$3.1/3.2 channels and the indicated KCTD proteins. The extracellular K^+ concentration was 100 mM. **b**, Experiments as in **a** but with oocytes co-expressing GABA$_B$, Ca$_v$2.2 channels and the indicated KCTD proteins; the bath solution contained 10 mM Ba^{2+}. Data points are maxima of currents elicited every 3 s by voltage steps from −100 mV to 0 mV (shown on the right for the indicated time points), successive GABA applications are denoted by the horizontal bars. The current scale is 0.1 μA. **c**, Bar graphs summarizing the relative desensitization determined for the indicated subunit combinations; wo KCTD, without KCTD. Data points are means and s.d. for 6–12 (GABA$_B$ + K$_{ir}$3.1/3.2), 8–13 (GABA$_B$ + Ca$_v$2.2) and 3–7 (GABA$_B$ + Ca$_v$2.1) experiments. Top right: time constants (τ_{desens}) and their relative contributions obtained from double-exponential fits to the K$_{ir}$3.1/3.2 current decay recorded in experiments as in **a** with KCTD12; data points are means and s.d. for 8 measurements.

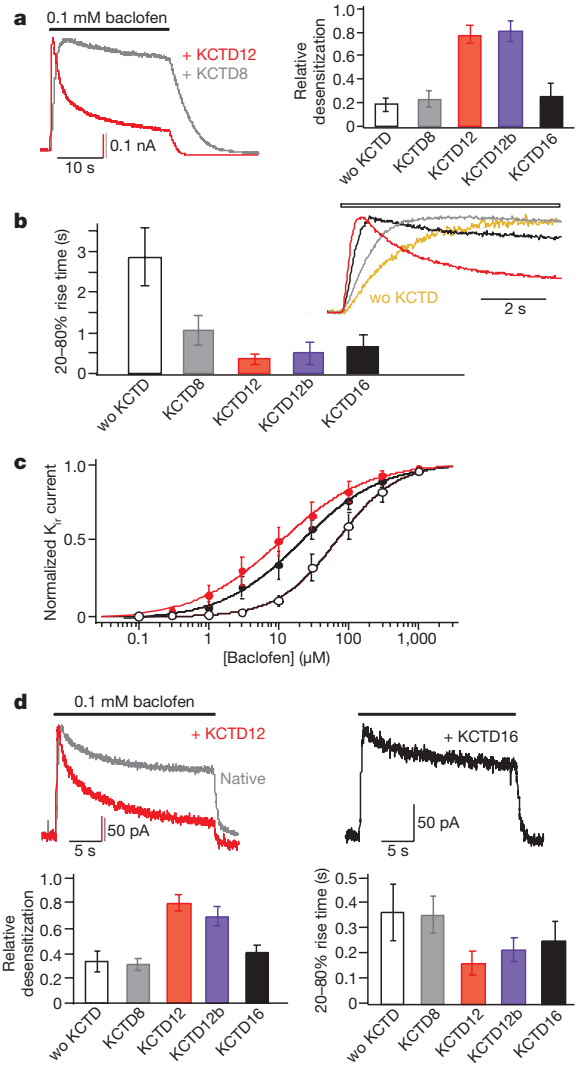

Figure 4 | KCTDs alter kinetics and agonist potency of the GABA$_B$ response in CHO cells and neurons. **a**, Left: K^+ currents through K$_{ir}$3.1/3.2 channels recorded at −50 mV in response to baclofen applications (0.1 mM) from whole CHO cells co-expressing GABA$_B$, K$_{ir}$3.1/3.2 channels and the indicated KCTD proteins; wo KCTD, without KCTD. The extracellular K^+ concentration was 2.5 mM. Right: summary plot as in Fig. 3c; data are means and s.d. for 6–31 experiments. **b**, The 20–80% rise time of K$_{ir}$3.1/3.2 currents activated by GABA$_B$ without or together with KCTD proteins. Data points are means and s.d. for 6–17 experiments. Inset: representative current onsets. **c**, Apparent dose–response relations obtained with GABA$_B$ (open circles) or with GABA$_B$ and KCTD proteins 12 (filled red circles) and 16 (filled black circles). Data points are means and s.d. for 7–13 experiments; lines are fits of a logistic function with values for EC_{50} values and Hill coefficients of 68.7 μM and 1.02 (GABA$_B$), 21.0 μM and 0.75 (GABA$_B$ + KCTD16), 9.9 μM and 0.63 (GABA$_B$ + KCTD12), respectively. **d**, Top: currents through K$_{ir}$3 channels recorded in experiments as in **a** from cultured hippocampal neurons without (native) or after transfection with KCTD12 (red trace) or KCTD16. Bottom: bar graphs summarizing relative desensitization (left) and onset (right) of the K$_{ir}$3 currents as in **a** and **b**; data points are means and s.d. for 7–38 experiments.

receptor response (Supplementary Figs 12 and 13). Taken together, these results indicate that KCTD proteins may extensively modify the G-protein signalling as well as the agonist potency at GABA$_B$ receptors.

The effects of KCTD on GABA$_B$ signalling are independent of cellular background or effector system but require tight assembly with the receptor core, in a similar manner to the interactions between auxiliary and pore-forming subunits of ion channels and transporters[10,19–21]. Accordingly, the KCTD action probably occurs at the GABA$_{B2}$ subunit, where KCTD tetramers are positioned to interact with both the C terminus and the heterotrimeric G protein[22]. The resulting increase in agonist potency and accelerated receptor–effector coupling will accentuate the GABA$_B$ response triggered either by agonists 'spilled over' from synapses on repetitive and/or synchronous firing[23] or by agonists released from synapses in response to single action potentials[24–26]. Together, the KCTD proteins endow GABA$_B$ receptors with subtype-specific properties of their G-protein signalling and thus provide a molecular basis for the functional diversity observed with native GABA$_B$ receptors.

METHODS SUMMARY

The proteomic approach, including the preparation of source material, affinity purifications and high-resolution mass spectrometry, as well as immunoelectron microscopy and electrophysiological recordings, were performed as described in refs 9–11.

Full Methods and any associated references are available in the online version of the paper at www.nature.com/nature.

Received 10 December 2009; accepted 24 February 2010.
Published online 18 April 2010.

1. Bettler, B., Kaupmann, K., Mosbacher, J. & Gassmann, M. Molecular structure and physiological functions of $GABA_B$ receptors. *Physiol. Rev.* **84,** 835–867 (2004).
2. Jones, K. A. *et al.* $GABA_B$ receptors function as a heteromeric assembly of the subunits $GABA_BR1$ and $GABA_BR2$. *Nature* **396,** 674–679 (1998).
3. Kaupmann, K. *et al.* Expression cloning of $GABA_B$ receptors uncovers similarity to metabotropic glutamate receptors. *Nature* **386,** 239–246 (1997).
4. Kaupmann, K. *et al.* $GABA_B$-receptor subtypes assemble into functional heteromeric complexes. *Nature* **396,** 683–687 (1998).
5. White, J. H. *et al.* Heterodimerization is required for the formation of a functional $GABA_B$ receptor. *Nature* **396,** 679–682 (1998).
6. Bonanno, G. & Raiteri, M. Multiple $GABA_B$ receptors. *Trends Pharmacol. Sci.* **14,** 259–261 (1993).
7. Cruz, H. G. *et al.* Bi-directional effects of $GABA_B$ receptor agonists on the mesolimbic dopamine system. *Nature Neurosci.* **7,** 153–159 (2004).
8. Deisz, R. A., Billard, J. M. & Zieglgänsberger, W. Presynaptic and postsynaptic $GABA_B$ receptors of neocortical neurons of the rat *in vitro*: differences in pharmacology and ionic mechanisms. *Synapse* **25,** 62–72 (1997).
9. Berkefeld, H. *et al.* BK_{Ca}-Cav channel complexes mediate rapid and localized Ca^{2+}-activated K^+ signaling. *Science* **314,** 615–620 (2006).
10. Schwenk, J. *et al.* Functional proteomics identify cornichon proteins as auxiliary subunits of AMPA receptors. *Science* **323,** 1313–1319 (2009).
11. Zolles, G. *et al.* Association with the auxiliary subunit PEX5R/Trip8b controls responsiveness of HCN channels to cAMP and adrenergic stimulation. *Neuron* **62,** 814–825 (2009).
12. Schuler, V. *et al.* Epilepsy, hyperalgesia, impaired memory, and loss of pre- and postsynaptic $GABA_B$ responses in mice lacking $GABA_{B1}$. *Neuron* **31,** 47–58 (2001).
13. Vigot, R. *et al.* Differential compartmentalization and distinct functions of $GABA_B$ receptor variants. *Neuron* **50,** 589–601 (2006).
14. Gassmann, M. *et al.* Redistribution of $GABA_{B1}$ protein and atypical $GABA_B$ responses in $GABA_{B2}$-deficient mice. *J. Neurosci.* **24,** 6086–6097 (2004).
15. Cox, J. & Mann, M. MaxQuant enables high peptide identification rates, individualized p.p.b.-range mass accuracies and proteome-wide protein quantification. *Nature Biotechnol.* **26,** 1367–1372 (2008).
16. Maurel, D. *et al.* Cell-surface protein–protein interaction analysis with time-resolved FRET and snap-tag technologies: application to GPCR oligomerization. *Nature Methods* **5,** 561–567 (2008).
17. Kulik, A. *et al.* Compartment-dependent colocalization of Kir3.2-containing K^+ channels and $GABA_B$ receptors in hippocampal pyramidal cells. *J. Neurosci.* **26,** 4289–4297 (2006).
18. Sodickson, D. L. & Bean, B. P. $GABA_B$ receptor-activated inwardly rectifying potassium current in dissociated hippocampal CA3 neurons. *J. Neurosci.* **16,** 6374–6385 (1996).
19. Arikkath, J. & Campbell, K. P. Auxiliary subunits: essential components of the voltage-gated calcium channel complex. *Curr. Opin. Neurobiol.* **13,** 298–307 (2003).
20. Jentsch, T. J. CLC chloride channels and transporters: from genes to protein structure, pathology and physiology. *Crit. Rev. Biochem. Mol. Biol.* **43,** 3–36 (2008).
21. Rettig, J. *et al.* Inactivation properties of voltage-gated K^+ channels altered by presence of β-subunit. *Nature* **369,** 289–294 (1994).
22. Duthey, B. *et al.* A single subunit (GB2) is required for G-protein activation by the heterodimeric $GABA_B$ receptor. *J. Biol. Chem.* **277,** 3236–3241 (2002).
23. Nicoll, R. A. My close encounter with $GABA_B$ receptors. *Biochem. Pharmacol.* **68,** 1667–1674 (2004).
24. Otis, T. S., De Koninck, Y. & Mody, I. Characterization of synaptically elicited $GABA_B$ responses using patch-clamp recordings in rat hippocampal slices. *J. Physiol. (Lond.)* **463,** 391–407 (1993).
25. Price, C. J., Scott, R., Rusakov, D. A. & Capogna, M. $GABA_B$ receptor modulation of feedforward inhibition through hippocampal neurogliaform cells. *J. Neurosci.* **28,** 6974–6982 (2008).
26. Tamas, G., Lorincz, A., Simon, A. & Szabadics, J. Identified sources and targets of slow inhibition in the neocortex. *Science* **299,** 1902–1905 (2003).

Supplementary Information is linked to the online version of the paper at www.nature.com/nature.

Acknowledgements We thank J. P. Adelman and H. R. Brenner for discussions and critical reading of the manuscript, and A. Haupt and K. Kaupmann for help with bioinformatics and shRNA experiments, respectively. This work was supported by grants from the Deutsche Forschungsgemeinschaft to B.F. (SFB 746/TP16; SFB 780/A3; EXC294) and to A.K. (SFB 780/A2), by grants from the Wellcome Trust (ISRF), the EU Synapse and the GACR (309/06/1304) to R.T., and by grants from the Swiss Science Foundation (3100A0-117816), the Fridericus Stiftung and the European Community's 7th Framework Programme (FP7/2007-2013) under Grant Agreement 201714 to B.B.

Author Contributions J.S., M.M., G.Z. and R.T. are equally contributing first authors. J.S., W.B., V.R., U.S. and B.F. performed proteomic analysis, biochemistry and evaluation of mass spectrometry. M.M., J.Y.T., M.G., J.T., T.F., M.R. and K.I. performed *in situ* hybridization, cellular biology, mouse work and KCTD antibody generation. G.Z., R.T., R.S. and M.R. conducted the electrophysiological recordings on oocytes, cultured cells and neurons. A.U., E.T. and A.K. performed electron microscopy. B.F., B.B. and U.S. initiated, designed and supervised the study. B.F. and B.B. wrote the manuscript.

Author Information Reprints and permissions information is available at www.nature.com/reprints. The authors declare no competing financial interests. Correspondence and requests for materials should be addressed to B.F. (bernd.fakler@physiologie.uni-freiburg.de) or B.B. (bernhard.bettler@unibas.ch).

METHODS

Molecular biology. The complementary DNAs used were all verified by sequencing and had the following GenBank accession numbers: Y10370 ($GABA_{B1}$), AJ011318 ($GABA_{B2}$), AY615967 (KCTD8), AY267461 (KCTD12), AL831725 (KCTD12b), NM_026135 (KCTD16), X57477.1 ($Ca_v2.1$), D14157.1 ($Ca_v2.2$), NM_017346.1 (Ca_v β1b), AF286488.1 (α2δ), NM_016574.2 (D2 receptor) and L14751.1 (P2Y2 receptor); the $K_{ir}3.1/3.2$ construct is as described[27].

In situ hybridizations were done with 10 µm cryosections of freshly frozen mouse tissue using digoxigenin-labelled riboprobes that were generated by transcription of cDNAs of mouse KCTDs 8, 12, 12b and 16 in the sense and antisense directions followed by alkaline hydrolysis of the probes to an average length of 200–400 bases[28]. Knockdown experiments were performed by transfection of cultured hippocampal neurons at DIV5 (day 5 *in vitro*) with pLL3.7 lentiviral vector expressing shRNAs under the mouse U6 promoter together with a cytomegalovirus–enhanced green fluorescent protein reporter cassette to monitor expression[29]. Efficiency of protein knockdown was assessed in western blots from HEK293 cells expressing Flag-tagged KCTD12. The shRNA constructs used had the following sequences: KCTD12-1, 5′-TGCCCGGACATCGTAGAGCTGAATGTGCTGTCTTCAGCTCTACGATGTCCGGGTTTTTTC-3′; sh-Control-1, 5′-TGGTATCTCTTCATAGCCTTATTCAAGAGATAAGGCTATGAAGAGATACTTTTTTC-3′; sh-Control-2, 5′-TGCAAGGCGATTACACTACCTTTCAAGAGAAGGTAGTGTAATCGCCTTGTTTTTTC-3′; interfering sequence stretches are underlined, TTTTTT is the polymerase III transcription termination sequence.

Biochemistry. Plasma-membrane-enriched protein fractions were prepared from freshly isolated rat or mouse brains and solubilized with ComplexioLyte buffers CL-75 or CL-91 (LOGOPHARM GmbH) as given in ref. 10; for rats and wild-type mice, preparations from at least 15 individual brains were pooled; for membrane fractions of knockout mice, preparations pooled from 10 brains were used.

BN–PAGE. Two-dimensional gel electrophoresis was performed as detailed in ref. 10 with CL-75 used for solubilization. For western blot analysis, the blot was split into two molecular mass ranges and analysed with anti-$GABA_{B1}$ (ref. 30) or anti-$GABA_{B2}$ (high-molecular-mass range; BD Transduction Laboratories) and anti-KCTD12 or anti-KCTD16 (low-molecular-mass range).

Affinity purification. Solubilized membrane fractions (2 mg, CL-91) were incubated for 2 h at 4 °C with 20 µg of immobilized affinity-purified anti-$GABA_{B1}$, anti-$GABA_{B2}$ (AB5394; Chemicon/Millipore), anti-KCTD12 (target sequence residues 145–166 of KCTD12 (accession no. AY267461); Supplementary Fig. 5), anti-KCTD16 (target sequence residues 8–23 of KCTD16 (accession no. NM_026135); Supplementary Fig. 5) or control IgG (Upstate/Millipore). After brief washing, bound proteins were eluted with Laemmli buffer (dithiothreitol added after elution), briefly run into SDS–PAGE gels and digested with trypsin as described[10]. For anti-Flag affinity purifications, cleared lysates of HEK293 cells were incubated overnight at 4 °C with immobilized anti-Flag antibody (Sigma). After separation by SDS–PAGE, purified proteins were analysed by western blot with the following antibodies: anti-Flag (Sigma), anti-haemagglutinin (Covance), anti-Myc (Roche) and peroxidase-coupled secondary antibodies (Amersham Biosciences).

In vivo protein synthesis and binding assays. Distinct domains of KCTD12 and $GABAB_{B2}$ were expressed in *Escherichia coli* BL21(DE3) as the following constructs (in modified pET16b, pET30 vectors): KCTD12-T1 (residues 27–131 of KCTD12 with an N-terminal His_6 tag), Tag-KCTD12-T1 (residues 27–131 of KCTD12 fused to a tag consisting of six histidine residues and the B1-binding domain of streptococcal protein G (His_6-GB1)), KCTD12-C_{term} (residues 202–327 fused to His_6-GB1 protein) and $GABA_{B2}$-C_{term} (residues 849–940 or 745–940 fused to His_6-GB1 protein). Proteins were purified to homogeneity by metal chelation affinity columns (Ni-Sepharose), anion exchange (MonoQ) and SEC (Superdex 200, 10/300 GL) run in Tris buffer (20 mM Tris-HCl, pH 8, 150 mM NaCl, 2 mM dithiothreitol). For binding studies, the respective purified proteins were mixed in roughly equimolar ratios and incubated for 30 min at room temperature (20–23 °C). After the addition of 0.01% Coomassie, G-250 complex formation was determined by native PAGE (12%) separation.

Analytical ultracentrifugation. Tag-KCTD12-T1 (0.25 and 0.5 mg ml^{-1}) dissolved in 150 mM NaCl and 20 mM Tris-HCl, pH 7.4 was loaded on a Beckman Optima-XLA (An60-Ti rotor) equipped with absorption optics. Sedimentation equilibrium runs were performed at 12,000 and 15,000 r.p.m. The molecular masses were determined by fitting the data with a single ideal species model[31].

Determination of stoichiometry. For determination of subunit stoichiometry in KCTD12-T1 + $GABA_{B2}$-$C_{745–940}$ complexes, SEC fractions were separated by SDS–PAGE and either stained with Sypro Orange (BioRad) for fluorescence-based analysis of protein bands or stained with silver and then digested with trypsin for quantitative LC–MS/MS analysis. The molar ratio of the two subunits was obtained either by comparing the fluorescence signals measured for each subunit and dividing this by the respective molecular mass (Sypro analysis), or by quantitative MS analysis (see below) with a purified chimaeric protein (fusion of KCTD12 and $GABA_{B2}$ expressed in *Xenopus* oocytes) as a 1:1 reference[10].

Mass spectrometry. LC–MS/MS analysis. High-resolution mass spectrometry was performed as detailed in ref. 10; database searches used the SwissProt database (Mammalia, release 56.8) supplemented with the TrEMBL entry Q8C7J6 for KCTD12b. Common variable modifications as well as one tryptic miscleavage were accepted; *m/z* peptide mass tolerance was ±10 p.p.m. and MS/MS tolerance was ±0.8 Da. The minimal Mascot peptide score was 20; protein identification and quantitative evaluation required at least two assigned peptides and a minimal normalized abundance value of 500.

Protein quantification. Two methods, relative peak volumes (rPV) and normalized protein abundance (normalized abundance; Fig. 1b and Supplementary Fig. 3), were used for protein quantification, both based on peak volumes (intensity of MS signal × retention time × (*m/z* width)) of individual tryptic peptides[10,15]. rPV values compare the amount of each protein identified in affinity purifications with the anti-$GABA_B$ and anti-KCTD antibodies from rat and mouse wild-type brains with the respective amount determined in affinity purifications either with IgGs (rat, rPV_{IgG}) or with the anti-$GABA_B$ and anti-KCTD antibodies from $GABA_B$ core subunit knockout animals (rPV_{ko}). rPV values are calculated as the median of the ratios of the six most consistent tryptic peptides of each protein; if the MS signal of a given peptide was not detected in the controls, the detection threshold of the spectrometer (3,000 volume units at the settings used) served as the denominator in rPV calculations. Any protein with an rPV value of more than 20 (affinity purifications from rat) or more than 10 (affinity purifications from mouse) were regarded as being specifically purified by the respective antibody.

Normalized abundance values compare the molar amounts of different proteins and are calculated as the sum of all assigned peak volumes divided by the number of MS-accessible amino acids (sequence of tryptic peptides with masses between 740 and 3,000 Da at the MS settings used). For KCTD12b, the normalized abundance value had to be corrected to account for the significant number of peptides shared with the markedly more abundant KCTD12; the actual contribution of KCTD12b was estimated from the mean peak volume ratio of KCTD12b-specific peptides versus KCTD12-specific peptides.

MS-based subunit stoichiometry in KCTD12-T1 + $GABA_{B2}$-$C_{745–940}$ complexes was determined as the median of the ratios calculated with the four top-ranked and calibrated (reference protein described above) peptides of $GABA_{B2}$-$C_{745–940}$ and the five top-ranked and calibrated peptides of KCTD12-T1 (a total of 20 ratios).

Sequence coverage. Sequence coverages (C_s) of $GABA_{B1a}$, $GABA_{B2}$ and the KCTD proteins were calculated as $C_s = N_i/(N_i + N_{an})$, where N_i is the number of amino-acid residues of the identified peptides (with a Mascot score of 20 or more) and N_{an} is the number of MS-accessible but not identified amino acids (see above) of the respective sequence.

Electron microscopy. Pre-embedding immunoelectron microscopy. Hippocampal sections of adult Wistar rats ($n = 8$) were treated for single immunogold labelling with affinity-purified anti-$GABA_{B1}$, anti-KCTD12 and anti-KCTD16 as described[32]. The secondary antibody was coupled with 1.4-nm gold particles to facilitate tissue penetration; silver enhancement (HQ Silver kit; Nanogold; Nanoprobes) was used to generate particles of detectable size (although variable in extent as a result of the random binding of the intensification kit).

SDS-digested freeze–fracture replica immunolabelling. Adult Wistar rats ($n = 6$) were processed for immunolabelling as described[33]. After digestion in 2.5% SDS solution, replicas were incubated first with anti-$GABA_{B1}$, anti-KCTD12 or anti-KCTD16 and subsequently with a 10-nm gold-coupled secondary antibody (1.30; British Biocell International).

Electrophysiological recordings and data analysis. Electrophysiological recordings from whole oocytes were performed at room temperature (22–24 °C) as described previously[10,34]. Currents were low-pass filtered at 1 kHz and sampled at 2 kHz; capacitive transients were compensated for with the compensation unit of the amplifier (TurboTec 10CX; npi) and a P/4 protocol. The extracellular solution was composed as follows (in mM): 100 KCl, 17.5 NaCl, 10 HEPES, 1.8 $CaCl_2$, pH 7.3 for $K_{ir}3.1/3.2$ channels, and 3 KCl, 102 NaCl, 10 HEPES and 10 $BaCl_2$, pH 7.3 for Ca_v channels, respectively. Solution exchange time was within about 1 s. Experiments on CHO cells stably expressing $GABA_B$ and on cultured hippocampal neurons were performed at room temperature (23–24 °C) 1–3 days or 1–2 weeks (DIV14–21) after a transfection, respectively. Cells were continuously superfused with an extracellular solution composed of (in mM): 145 NaCl, 2.5 KCl, 1 $MgCl_2$, 2 $CaCl_2$, 10 HEPES, 25 glucose, pH 7.3, 323 mosM. Neurons were superfused with extracellular solution supplemented with 5 µM 6,7-dinitroquinoxaline-2,3-dione, 0.5 µM tetrodotoxin, 0.3 µM strychnine, 100 µM picrotoxin, 5 µM D-CPP. Patch pipettes had resistances between 3 and 4 MΩ when filled with

intracellular solution composed of (in mM) 107.5 potassium gluconate, 32.5 KCl, 10 HEPES, 5 EGTA, 4 MgATP, 0.6 NaGTP, 10 Tris phosphocreatine; pH 7.2, 297 mosM. Series resistance (less than 5 MΩ) was compensated for by 80%. $GABA_B$ responses were evoked by fast application of baclofen[35] and recorded with an Axopatch 200B patch-clamp amplifier; filtering and sampling frequencies were set to 1 and 5 kHz, respectively.

Relative desensitization was calculated as the percentage decrease in effect (increase for K_{ir} currents, decrease for Ca_v currents) measured during prolonged agonist applications (60 or 25 s): $100 \times [1 - (\text{agonist-induced effect at the end of application})/(\text{maximal agonist-induced effect})]$. Desensitization time constants were derived from double-exponential fits to the decay phase of $K_{ir}3.1/3.2$ currents during agonist application. Curve fitting and further data analysis were performed with Igor Pro 4.05A Carbon; data are given as means and s.d. as indicated in the text and figure legends. Statistical significance was assessed by analysis of variance with Dunnett's multiple comparison test.

27. Wischmeyer, E. *et al.* Subunit interactions in the assembly of neuronal Kir3.0 inwardly rectifying K^+ channels. *Mol. Cell. Neurosci.* **9,** 194–206 (1997).
28. Schaeren-Wiemers, N. & Gerfin-Moser, A. A single protocol to detect transcripts of various types and expression levels in neural tissue and cultured cells: *in situ* hybridization using digoxigenin-labelled cRNA probes. *Histochemistry* **100,** 431–440 (1993).
29. Rubinson, D. A. *et al.* A lentivirus-based system to functionally silence genes in primary mammalian cells, stem cells and transgenic mice by RNA interference. *Nature Genet.* **33,** 401–406 (2003).
30. Engle, M. P. *et al.* Spinal nerve ligation does not alter the expression or function of $GABA_B$ receptors in spinal cord and dorsal root ganglia of the rat. *Neuroscience* **138,** 1277–1287 (2006).
31. Rivas, G., Stafford, W. & Minton, A. P. Characterization of heterologous protein–protein interactions using analytical ultracentrifugation. *Methods* **19,** 194–212 (1999).
32. Kulik, A. *et al.* Subcellular localization of metabotropic $GABA_B$ receptor subunits $GABA_{B1a/b}$ and $GABA_{B2}$ in the rat hippocampus. *J. Neurosci.* **23,** 11026–11035 (2003).
33. Masugi-Tokita, M. *et al.* Number and density of AMPA receptors in individual synapses in the rat cerebellum as revealed by SDS-digested freeze-fracture replica labeling. *J. Neurosci.* **27,** 2135–2144 (2007).
34. Zolles, G. *et al.* Pacemaking by HCN channels requires interaction with phosphoinositides. *Neuron* **52,** 1027–1036 (2006).
35. Dittert, I. *et al.* Improved superfusion technique for rapid cooling or heating of cultured cells under patch-clamp conditions. *J. Neurosci. Methods* **151,** 178–185 (2006).